Journal of Molecular Liquids 251 (2018) 212–217

Contents lists available at ScienceDirect

Journal of Molecular Liquids

journal homepage: www.elsevier.com/locate/molliq

A highly selective and sensitive voltammetric sensor with molecularly imprinted polymer based silver@gold nanoparticles/ionic liquid modified glassy carbon electrode for determination of ceftizoxime

Murat Beytur [a], Faruk Kardaş [b], Onur Akyıldırım [c], Abdullah Özkan [d], Bahar Bankoğlu [e], Haydar Yüksek [a], Mehmet Lütfi Yola [f,*], Necip Atar [g,*]

[a] Department of Chemistry, Faculty of Science and Letters, Kafkas University, Kars, Turkey
[b] Department of Science Education, Faculty of Education, Erzincan University, Erzincan, Turkey
[c] Department of Chemical Engineering, Faculty of Engineering and Architecture, Kafkas University, Kars, Turkey
[d] Iskenderun Technical University, Faculty of Engineering and Natural Sciences, Department of Petroleum and Natural Gas, Hatay, Turkey
[e] Iskenderun Technical University, Science and Technology Application and Research Laboratory, Hatay, Turkey
[f] Iskenderun Technical University, Faculty of Engineering and Natural Sciences, Department of Biomedical Engineering, Hatay, Turkey
[g] Pamukkale University, Faculty of Engineering, Department of Chemical Engineering, Denizli, Turkey

ARTICLE INFO

Article history:
Received 27 November 2017
Received in revised form 12 December 2017
Accepted 13 December 2017
Available online 14 December 2017

Keywords:
Ceftizoxime
Core@shell nanoparticles
Molecularly imprinted polymer
Characterization

ABSTRACT

Ceftizoxime (CFX) is used to reduce the infection caused by both gram-negative and gram-positive bacteria. In this report, silver@gold nanoparticles (Ag@AuNPs) involved in 5-(5-bromo-2-hydroxybenzylidenamino)-2-mercaptobenzimidazole (ILs) was firstly synthesized. After that, CFX imprinted glassy carbon electrode (GCE) was prepared. The formation of the surfaces was characterized by scanning electron microscope (SEM), transmission electron microscope (TEM), electrochemical impedance spectroscopy (EIS) and x-ray photoelectron spectroscopy (XPS). CFX imprinted electrochemical surface was formed in the presence of 100.0 mM phenol containing 25.0 mM CFX as template. The linearity range and the detection limit (LOD) of the developed nanosensor were calculated as 1.0×10^{-9} - 1.0×10^{-11} M and 2.0×10^{-12} M, respectively.

1. Introduction

Ceftizoxime (CFX) is important cephalosporin antibiotic that is active against aerobic both gram-negative and gram-positive bacteria and reduces the putrefaction [1–3]. CFX is widely utilized in the therapy of infection including skin and mild texture infection, bone and joint infection and other ventral infections [4–7]. The quantitative determination of antibiotics and analgesics in biological fluids is necessary for drug metabolism. There are several methods such as spectrophotometry [3] and chromatography [8,9] for determination of CFX. Nonetheless, these methods have difficult extraction steps for real sample analysis. In addition, there are much material consumption. Thus, the fast and sensitive analytical methods based on nanocomposite are urgently needed [10,11]. Especially, the significant developments are carried out in adsorption studies, sensitive and selective nanosensors [12–20].

The molecular imprinting technique is based on polymerization around template [21,22]. The specific cavities to target molecule are easily formed in the polymerization process. Hence, we can create selective and sensitive sensor based on molecularly imprinting polymer (MIP) [23]. Up to now, there is no original work on the electrochemical detection of CFX by Ag@Au NPs involved in ILs modified GCE with MIP. The nanocomposite was characterized by SEM, TEM, CV, EIS and XPS. After that, MIP/Ag@Au NPs/ILs/GCE were developed in the presence of 100.0 mM phenol and 25.0 mM CFX. 1.0×10^{-12} - 1.0×10^{-9} M and 2.0×10^{-13} were calculated for linearity range and LOD, respectively. Finally, the electrodes were applied to pharmaceutical samples for CFX analysis.

2. Experimental

2.1. Materials

Chemical reagents in the present study were purchased from Merck AG, Aldrich and Fluka. Melting point was determined in open glass capillary using a Stuart melting point SMP30 apparatus and is uncorrected. The IR spectra were obtained on an ALPHA-P BRUKER FT-IR spectrometer. ^{1}H and ^{13}C NMR spectra were recorded in deuterated dimethyl sulfoxide with TMS as internal standard using a Varian spectrometer at 400 MHz and 100 MHz, respectively. In addition, ascorbic acid (AA) and dopamine (DA) stock aqueous solutions (1.0 mM) were prepared in Britton-Robinson (BR) buffer solution (BR) (0.04 M, pH 3.0). IviumStat (US) equipped with C3 cell stand was used for obtaining

* Corresponding authors.
E-mail addresses: mlutfi.yola@iste.edu.tr (M.L. Yola), natar@pau.edu.tr (N. Atar).

https://doi.org/10.1016/j.molliq.2017.12.060
0167-7322/

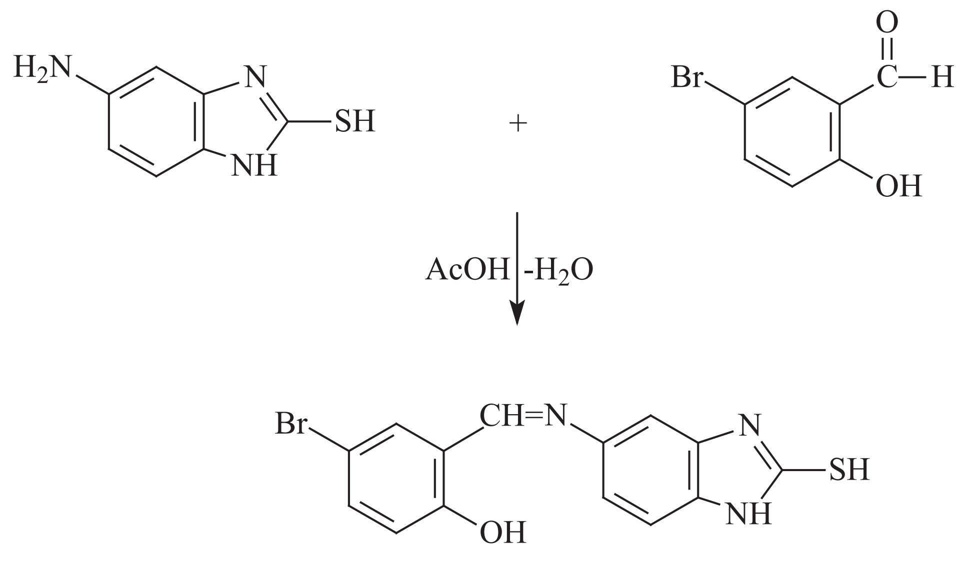

Scheme 1. Synthesis route of compound **1**.

differential pulse voltammogram (DPV), cyclic voltammogram and electrochemical impedance curves. PHI 5000 Versa Probe (FULVAC-PHI, Inc., Japan/USA) was utilized for XPS. TEM images were obtained on a JEOL 2100 HRTEM and ZEISS EVO 50 analytic microscope (Germany) model was performed for SEM images (Scheme 1).

2.2. Synthesis of 5-(5-bromo-2-hydroxybenzylidenamino)-2-mercaptobenzimidazole

5-Amino-2-mercaptobenzimidazole (0.005 mol) was dissolved in acetic acid (20 mL) and treated with 5-bromo-2-hydroxybenzaldehyde (0.005 mol), and then evaporated at 50–55 °C *in vacuo*. Several recrystallization of the residue from ethanol gave pure compound 5-(5-bromo-2-hydroxybenzylidenamino)-2-mercaptobenzimidazole **1** as orange color crystals. Yield: 1.55 g (89%); mp: 289 °C; IR (KBr, υ, cm^{-1}): 3275 (OH), 3124 (NH), 2562 (SH), 1602, 1564 (C=N), 777 (1,2-disubstituted benzenoid ring); ^{1}H NMR (400 MHz, DMSO d_6): δ 6.92 (d, 1H, Ar—H, J = 8.8 Hz), 7.29–7.12 (m, 3H, Ar—H), 7.51 (dd, 1H, Ar—H, J = 8.8, 2.0 Hz), 7.85 (d, 1H, Ar—H, J = 2.0 Hz), 8.96 (s, 1H, N=CH), 12.68 (s, 1H, OH), 12.75 (s, 1H, SH), 13.16 (s, 1H, NH); ^{13}C NMR (100 MHz, DMSO d_6): δ 101.53 (arom-C), 109.83 (2C), 117.32 (arom-C), 118.91 (arom-C), 121.22 (arom-C), 131.71 (arom-C), 133.09 (arom-C), 133.93 (arom-C), 135.11 (arom-C), 142.64 (arom-C), 159.20 (N=CH), 160.55 (arom-C-OH), 169.14 (C-SH).

2.3. Synthesis of the nanocomposite and preparation of the modified electrode

Ag@Au NPs was prepared according to the procedure [24]. First of all, 1 mM 250 mL of $AgNO_3$ solution was mixed with 40 mM of sodium

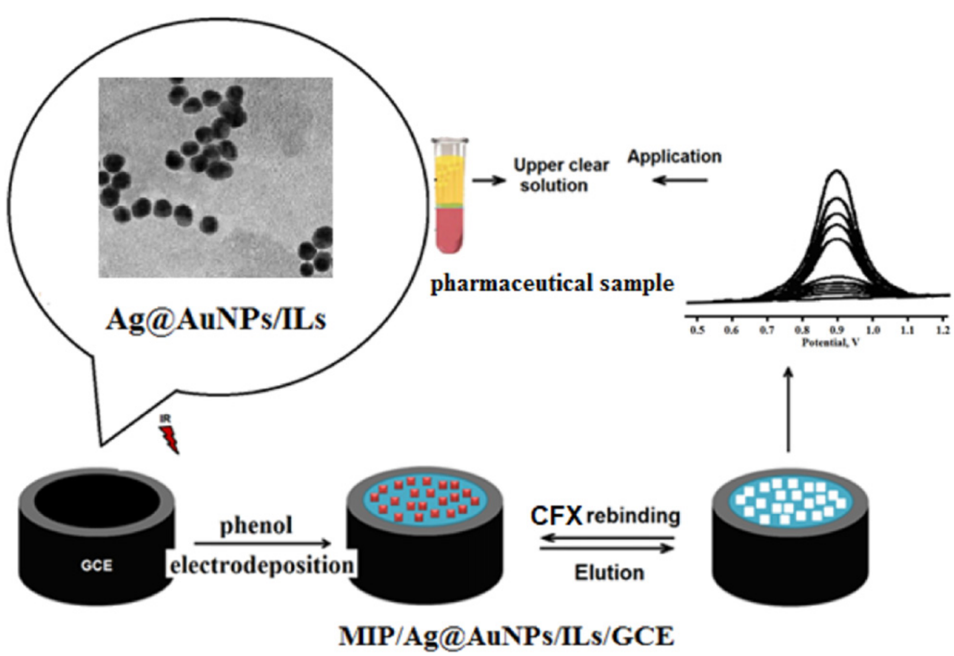

Scheme 2. The procedure of MIP/Ag@AuNPs/ILs/GCE.

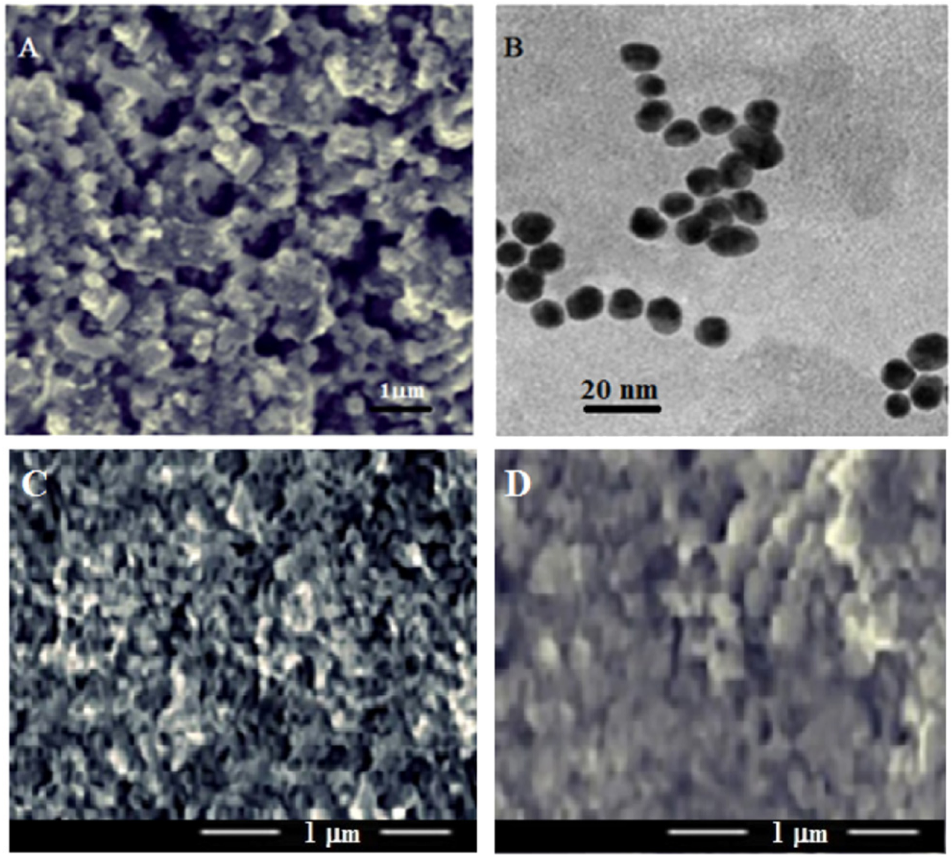

Fig. 1. (A) SEM image of Ag@AuNPs/ILs/GCE surface, (B) TEM image of Ag@AuNPs/ILs, (C) SEM images of the MIP electrode surface and (D) the NIP electrode surface.

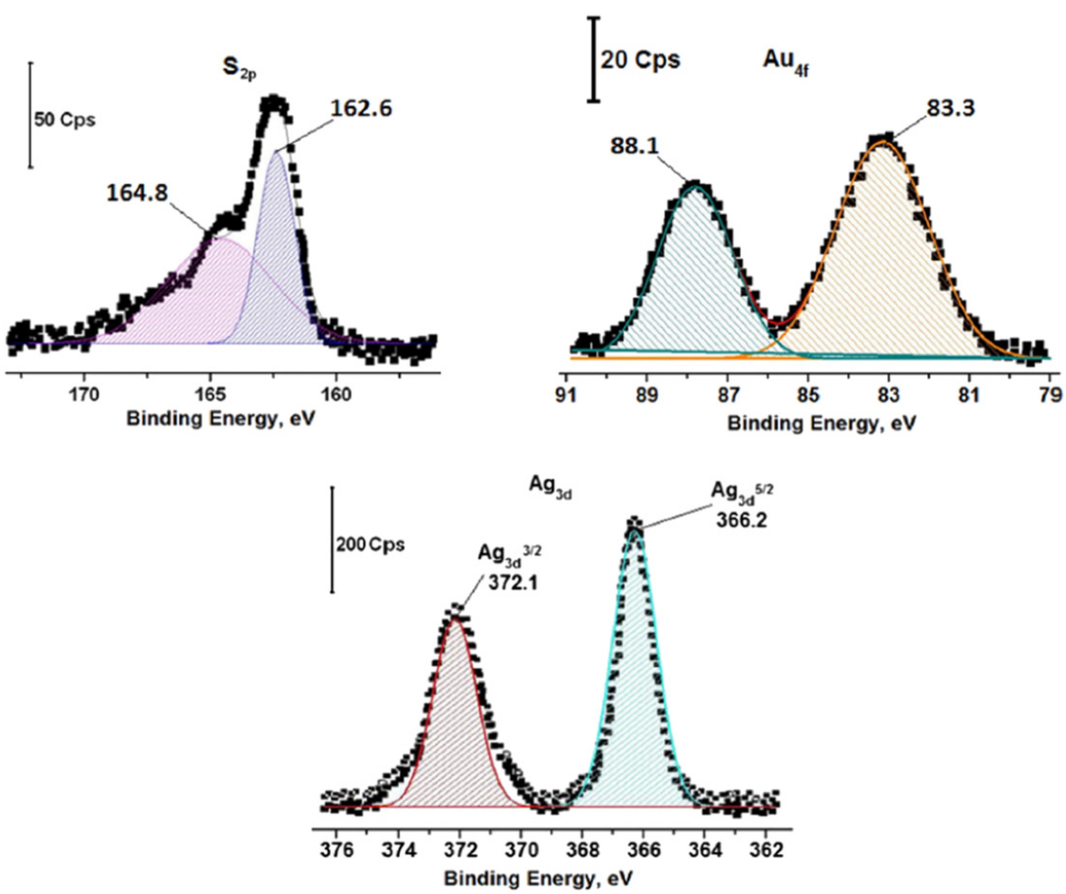

Fig. 2. Curve-fitted (XPS) spectra of S2p, Ag3d and Au4f.

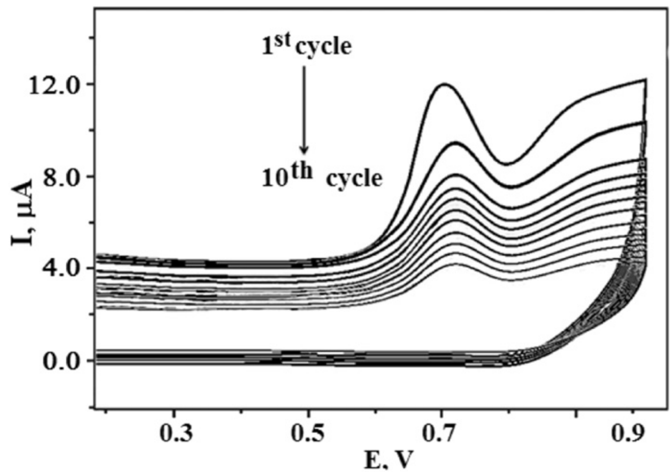

Fig. 3. Cyclic voltammogram for the electrochemical polymerization of phenol (100 mM) in the presence of CFX (25 mM) in BR (pH 3.0) at scan rate of 100 mV s^{-1} for 10 cycles.

citrate (20 mL) under room temperature, and then 110 mM of $NaBH_4$ (5 mL) was added to the mixture (Ag NPs). After that, 0.45 mM of $HAuCl_4$ (50 mL) and 6.25 mM of $NH_2OH{\cdot}HCl$ solutions (50 mL) were added drop by drop to the as-prepared AgNPs solution under room temperature. Ag@Au NPs was prepared by stirring the mixture until the color was turned into lilac from pale yellow [24]. Ag@Au NPs/ILs modified GCE was developed according to the report [25]. The reference and counter electrodes are Ag/AgCl(aq) and Pt wire, respectively.

2.4. Procedure of CFX imprinted electrodes and CFX removal

The procedure of CFX imprinted Ag@AuNPs/ILs/GCE electrode (MIP/Ag@Au NPs/ILs/GCE) is schematically explained (Scheme 2). After the preparation of Ag@Au NPs/ILs/GCE as working electrode, 100.0 mM phenol containing 25.0 mM CFX in 0.04 M BR (pH 3.0) was prepared in voltammetric cell. The potential (from 0.0 V to + 1.0 V) was applied to working electrode by cyclic voltammetry (CV) for 10 cycles. The other imprinted electrodes were prepared with same procedure. The imprinted electrode based on Ag@Au NPs/ILs/GCE without CFX (NIP/Ag@AuNPs/ILs/GCE) was also developed to investigate the selectivity of imprinting. 1.0 M NaCl solution was used for CFX removal on electrode surface. The removal procedure was performed according to the literature [26]. After the potential (from 0.5 V to + 1.2 V) was applied to working electrode, the voltammograms were evaluated for CFX detection.

3. Results and discussion

3.1. Characterization and electrochemical studies

The morphology of the Ag@AuNPs/ILs/GCE surface was characterized by SEM. Fig. 1A shows dense layers on the electrode surface, indicating the successful binding of Ag@AuNPs/ILs. The presence of Ag@AuNPs on nano-linked with ILs is confirmed on Fig. 1B. According to the structure analysis, the average diameters with 20–25 nm are obtained for Ag@AuNPs. Fig. 1B shows the TEM image of Ag@AuNPs/ILs. In Ag@AuNPs morphology, the darker nucleus is assigned to AgNPs and the lighter shell is assigned to AuNPs. The layer of intensive CFX imprinted polymer is seen on SEM analysis (Fig. 1C). According to Fig. 1C, the mean cavity sizes are 50–80 nm. The less porous structure of NIP surface was seen in comparison with MIP surface (Fig. 1D).

XPS characterization shows the formation of Ag@AuNPs/ILs/GCE (Fig. 2). S2p spectrum was curve-fitted with two components by a doublet 2p1/2 and 2p3/2 signals [27]. The peak at 162.6 eV confirmed Au NPs were linked to S atoms. Ag3d curve is characterized by a doublet 3d5/2 and 3d3/2 signals at 366.2 and 372.1 eV, respectively, indicating the existence of Ag NPs. The peak signals at 83.3 and 88.1 eV are corresponded to Au 4f7/2 and 4f5/2, respectively, showing the functionalization of Au NPs with sulfur atoms [27].

During the first scan, the oxidation potential of monomer was 0.68 V (Fig. 3). The current signals at 0.68 V diminished with subsequent scans. They vanished at 10th cycle on Ag@AuNPs/ILs/GCE. Thus, we think that CFX imprinted electrode is successfully formed on Ag@AuNPs/ILs/GCE.

Fig. 4A shows the impedance plot of the modified electrodes. The obtained charge transfer resistance (Rct) values of the prepared electrodes are 88 Ω (curve d), 112 Ω (curve c), 143 Ω (curve b) and 184 Ω (curve a), respectively. According to Fig. 4B, After phenol's polymerization on the modified surface, Rct value was obtained as 105 Ω (curve a of Fig. 4B). This situation indicated the obstruction effect of MIP film. After CFX removal on MIP/Ag@AuNPs/ILs/GCE, the analyte molecule's recognition sites appeared again and Rct value decreased (curve c of Fig. 4B). When CFX's rebinding on electrode, the value of Rct increased to 56 Ω (curve b of Fig. 4B).

The curve a of Fig. 5A shows the signal of MIP/Ag@AuNPs/ILs/GCE without template in 0.04 M BR solution (pH 3.0). As shown in Fig. 5A, there is no signal observation on the voltammogram (curve a). However, the prepared nanosensor demonstrates an obvious current signal at 0.90 V (curve c of Fig. 5A). In addition, NIP/Ag@AuNPs/ILs/GCE was prepared at the same conditions without template molecule. The small signal was observed in curve b of Fig. 5A. Finally, different molecular imprinted electrodes were prepared (Fig. 5B). According to Fig. 5B, the prepared MIP/Ag@AuNPs/ILs/GCE shows the most catalytic effect in comparison the other imprinted electrodes. Fig. 5C indicated the relation between current signals and CFX concentrations. The regression equation is $y(\mu A) = 9.55 \times (nM) - 0.041$. The quantification limit

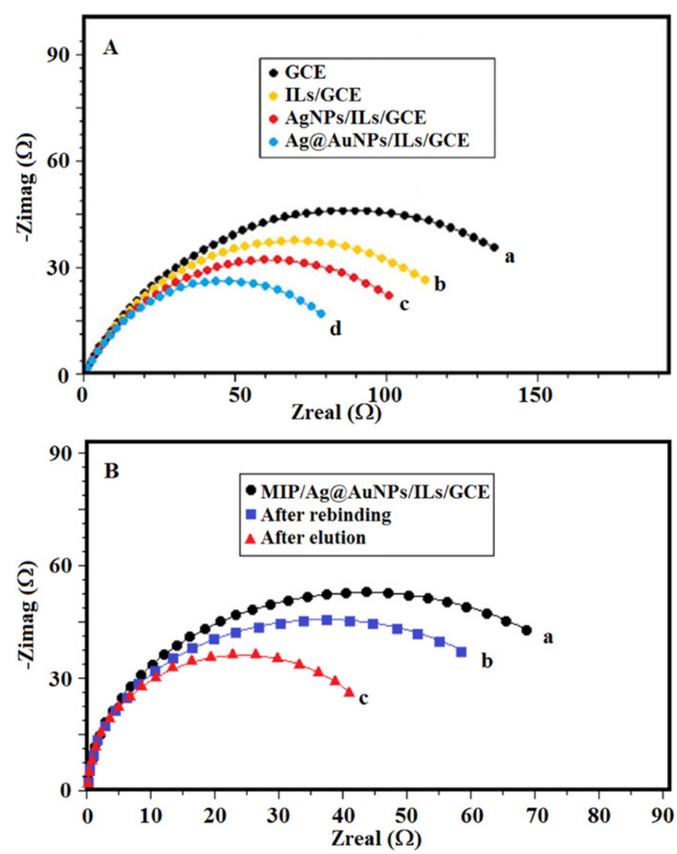

Fig. 4. (A) Fitting of impedance spectrum for 1.0 mM $[Fe(CN)_6]^{3-/4-}$ (1:1) in 0.1 M KCl at bare GCE (curve a), ILs/GCE (curve b), AgNPs/ILs/GCE (curve c) and Ag@AuNPs/ILs/GCE (curve d); (B) EIS of (a) MIP/Ag@AuNPs/ILs/GCE (with template molecule); (b) MIP/Ag@AuNPs/ILs/GCE (after rebinding of 1.0 nM CFX); (c) MIP/Ag@AuNPs/ILs/GCE (removing template) in 1.0 mM $[Fe(CN)_6]^{3-/4-}$ solution in 0.1 M KCl.

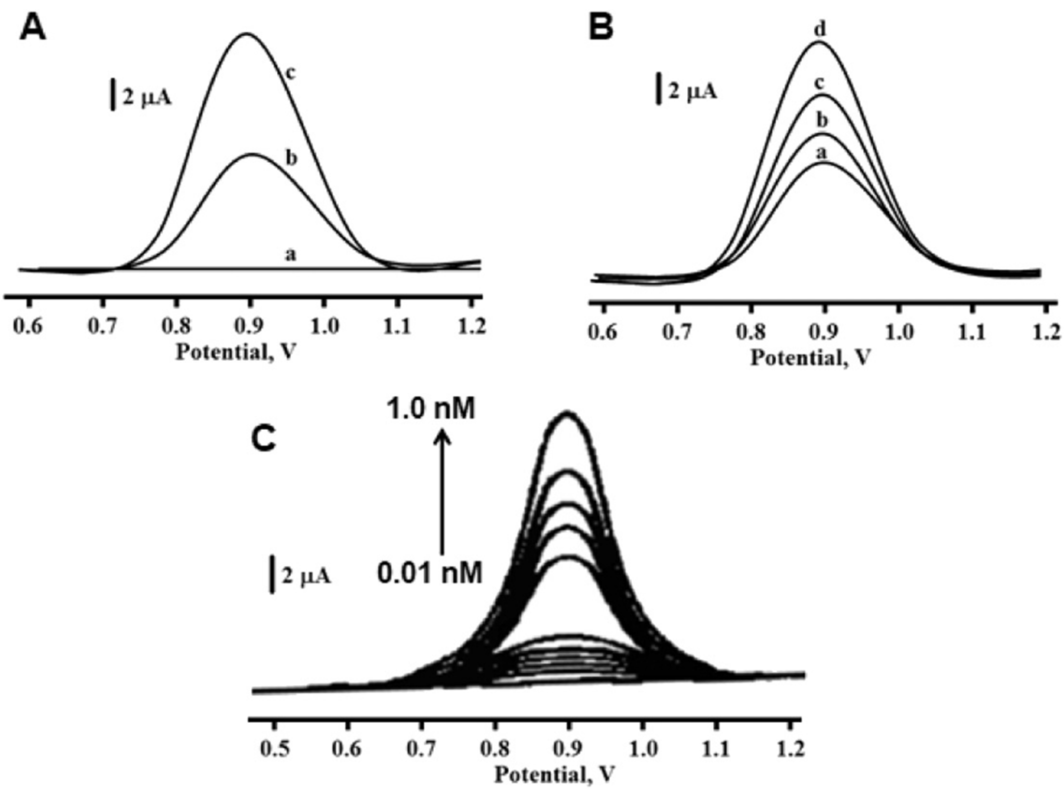

Fig. 5. (A) The differential pulse voltammograms of the electrodes in present work: (a) MIP/Ag@AuNPs/ILs/GCE in blank buffer solution, (b) NIP/Ag@AuNPs/ILs/GCE after rebinding of 1.0 nM CFX, (c) MIP/Ag@AuNPs/ILs/GCE after rebinding of 1.0 nM CFX; (B) DPVs of different molecular imprinted electrodes after rebinding of 1.0 nM CFX (a) bare GCE; (b) ILs/GCE; (c) Ag/ILs/GCE; (d) Ag@AuNPs/ILs/GCE; (C) The differential pulse voltammograms with different CFX concentrations (from 0.01 nM to 1.0 nM) in pH 3.0 of BR.

(LOQ) and LOD for CFX were obtained as 1.0×10^{-11} M and 2.0×10^{-12} M, respectively.

3.2. Selectivity, stability, repeatability and reproducibility of MIP/Ag@AuNPs/ILs/GCE

The selectivity experiments in pharmaceutical sample were performed in the presence of CFX, AA and DA. According to Fig. 6, the nanosensor in present work was 10.0, 20.0 and 40.0 times selective towards CFX in comparison with AA and DA. Hence, we can say that the developed nanosensor has good selectivity. The one sensor was prepared for the stability of MIP/Ag@AuNPs/ILs/GCE. After that, the current signals were measured for 60 days. The mean value of current signals is 95.03% of the first current signal. Thus, the nanosensor in present work is used in long-term for pharmaceutical sample analysis. For the repeatability of MIP/Ag@AuNPs/ILs/GCE, DPVs of twenty five were obtained in the presence of 1.0 nM CFX. According to results, MIP/Ag@AuNPs/ILs/GCE had the repeated signals at about 21.3 μA. Consequently, the matrix presence in pharmaceutical samples cannot importantly affect the selective analysis of CFX.

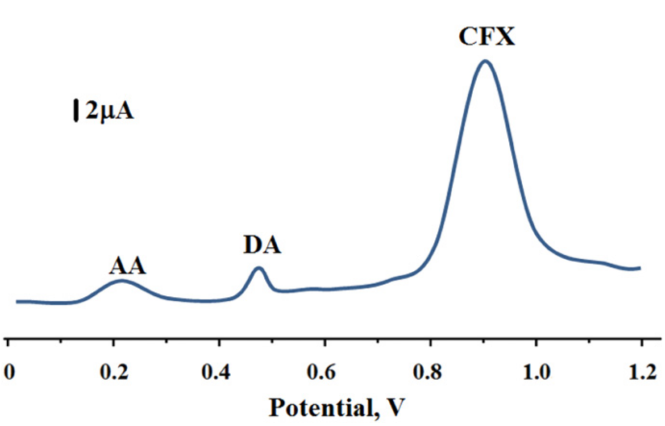

Fig. 6. The differential pulse voltammograms related to 1.0 nM CFX, AA and DA in pharmaceutical sample.

4. Conclusion

In this report, novel molecular imprinted sensor based on silver@gold nanoparticles involved in 5-(5-bromo-2-hydroxybenzylidenamino)-2-mercaptobenzimidazole was developed and applied for ceftizoxime detection in pharmaceutical sample. The prepared nanomaterial and surfaces were well characterized by using TEM, SEM, XPS, DPV and EIS. 1.0×10^{-9} - 1.0×10^{-11} and 2.0×10^{-12} M were founded as the linearity range and the detection limit. Due to these results, we can say that the electrochemical imprinted sensor was utilized for the determination of significant cephalosporin antibiotics without interference.

References

[1] S. Shahrokhian, S. Ranjbar, M. Ghalkhani, Modification of the electrode surface by ag nanoparticles decorated nano diamond-graphite for voltammetric determination of ceftizoxime, Electroanalysis 28 (2016) 469–476.
[2] S.K. Yadav, B. Agrawal, R.N. Goyal, AuNPs-poly-DAN modified pyrolytic graphite sensor for the determination of cefpodoxime proxetil in biological fluids, Talanta 108 (2013) 30–37.
[3] X.-B. Zhang, Y.-C. Feng, C.-Q. Hu, Feasibility and extension of universal quantitative models for moisture content determination in beta-lactam powder injections by near-infrared spectroscopy, Anal. Chim. Acta 630 (2008) 131–140.
[4] R. Ojani, J.-B. Raoof, S. Zamani, A novel sensor for cephalosporins based on electrocatalytic oxidation by poly(o-anisidine)/SDS/Ni modified carbon paste electrode, Talanta 81 (2010) 1522–1528.

[5] L. Wang, X. Zheng, W. Zhong, J. Chen, J. Jiang, P. Hu, Validation and application of an LC-MS-MS method for the determination of ceftizoxime in human serum and urine, J. Chromatogr. Sci. 54 (2016) 713–719.
[6] S. Sanli, N. Sanli, M. Gumustas, S.A. Ozkan, N. Karadas, H.Y. Aboul-Enein, Simultaneous estimation of ceftazidime and ceftizoxime in pharmaceutical formulations by HPLC method, Chromatographia 74 (2011) 549–558.
[7] T.K. Sar, T.K. Mandal, I. Samanta, A. Rahaman, A.K. Chakraborty, Determination of ceftriaxone in plasma and ceftizoxime in milk of mastitic cows following single dose intravenous administration, Indian J. Anim. Sci. 80 (2010) 1182–1184.
[8] I. Ali, Z.A. Al-Othman, H.Y. Aboul-Enein, K. Saleem, I. Hussain, Fast analysis of third-generation cephalosporins in human plasma by SPE and HPLC methods, LCGC N. Am. 29 (2011).
[9] H.Y.A.-E. Imran Ali, Vinod K. Gupta, Nano Chromatography and Capillary Electrophoresis: Pharmaceutical and Environmental Analyses, Wiley & Sons, Hoboken, USA, 2009 1–270.
[10] F. Kardaş, M. Beytur, O. Akyıldırım, H. Yüksek, M.L. Yola, N. Atar, Electrochemical detection of atrazine in wastewater samples by copper oxide (CuO) nanoparticles ionic liquid modified electrode, J. Mol. Liq. 248 (2017) 360–363.
[11] M.L. Yola, C. Göde, N. Atar, Molecular imprinting polymer with polyoxometalate/carbon nitride nanotubes for electrochemical recognition of bilirubin, Electrochim. Acta 246 (2017) 135–140.
[12] C. Göde, M.L. Yola, A. Yılmaz, N. Atar, S. Wang, A novel electrochemical sensor based on calixarene functionalized reduced graphene oxide: application to simultaneous determination of Fe(III), Cd(II) and Pb(II) ions, J. Colloid Interface Sci. 508 (2017) 525–531.
[13] Ö.A. Yokuş, F. Kardaş, O. Akyildirim, T. Eren, N. Atar, M.L. Yola, Sensitive voltammetric sensor based on polyoxometalate/reduced graphene oxide nanomaterial: application to the simultaneous determination of l-tyrosine and l-tryptophan, Sensors Actuators B Chem. 233 (2016) 47–54.
[14] M.L. Yola, V.K. Gupta, N. Atar, New molecular imprinted voltammetric sensor for determination of ochratoxin A, Mater. Sci. Eng. C 61 (2016) 368–375.
[15] F. Tahernejad-Javazmi, M. Shabani-Nooshabadi, H. Karimi-Maleh, Analysis of glutathione in the presence of acetaminophen and tyrosine via an amplified electrode with MgO/SWCNTs as a sensor in the hemolyzed erythrocyte, Talanta 176 (2018) 208–213.
[16] Z. Keivani, M. Shabani-Nooshabadi, H. Karimi-Maleh, An electrochemical strategy to determine thiosulfate, 4-chlorophenol and nitrite as three important pollutants in water samples via a nanostructure modified sensor, J. Colloid Interface Sci. 507 (2017) 11–17.
[17] I. Ali, Z.A. Alothman, A. Alwarthan, Uptake of propranolol on ionic liquid iron nanocomposite adsorbent: kinetic, thermodynamics and mechanism of adsorption, J. Mol. Liq. 236 (2017) 205–213.
[18] I. Ali, O.M.L. Alharbi, Z.A. Alothman, A.Y. Badjah, A. Alwarthan, A.A. Basheer, Artificial neural network modelling of amido black dye sorption on iron composite nano material: kinetics and thermodynamics studies, J. Mol. Liq. 250 (2018) 1–8.
[19] I. Ali, Z.A. Al-Othman, A. Alwarthan, Synthesis of composite iron nano adsorbent and removal of ibuprofen drug residue from water, J. Mol. Liq. 219 (2016) 858–864.
[20] I. Ali, Z.A. Al-Othman, O.M.L. Alharbi, Uptake of pantoprazole drug residue from water using novel synthesized composite iron nano adsorbent, J. Mol. Liq. 218 (2016) 465–472.
[21] M.L. Yola, T. Eren, N. Atar, A molecular imprinted voltammetric sensor based on carbon nitride nanotubes: application to determination of melamine, J. Electrochem. Soc. 163 (2016) B588–B593.
[22] O. Akyıldırım, F. Kardaş, M. Beytur, H. Yüksek, N. Atar, M.L. Yola, Palladium nanoparticles functionalized graphene quantum dots with molecularly imprinted polymer for electrochemical analysis of citrinin, J. Mol. Liq. 243 (2017) 677–681.
[23] M.L. Yola, N. Atar, Electrochemical detection of atrazine by platinum nanoparticles/carbon nitride nanotubes with molecularly imprinted polymer, Ind. Eng. Chem. Res. 56 (2017) 7631–7639.
[24] N. Atar, T. Eren, B. Demirdögen, M.L. Yola, M.O. Çağlayan, Silver, gold, and silver@gold nanoparticle-anchored L-cysteine-functionalized reduced graphene oxide as electrocatalyst for methanol oxidation, Ionics 21 (2015) 2285–2293.
[25] M.L. Yola, C. Göde, N. Atar, Determination of rutin by $CoFe_2O_4$ nanoparticles ionic liquid nanocomposite as a voltammetric sensor, J. Mol. Liq. 246 (2017) 350–353.
[26] M.L. Yola, N. Atar, T. Eren, H. Karimi-Maleh, S. Wang, Sensitive and selective determination of aqueous triclosan based on gold nanoparticles on polyoxometalate/reduced graphene oxide nanohybrid, RSC Adv. 5 (2015) 65953–65962.
[27] M.L. Yola, T. Eren, N. Atar, A sensitive molecular imprinted electrochemical sensor based on gold nanoparticles decorated graphene oxide: application to selective determination of tyrosine in milk, Sensors Actuators B Chem. 210 (2015) 149–157.